J Neurophysiol 89: 2667–2677, 2003.
First published January 29, 2003; 10.1152/jn.00742.2002.

Kinematics and Kinetics of Multijoint Reaching in Nonhuman Primates

Kirsten M. Graham,[1] Kimberly D. Moore,[1] D. William Cabel,[1] Paul L. Gribble,[1] Paul Cisek,[2] and Stephen H. Scott[1]

[1]*Department of Anatomy and Cell Biology, Centre for Neuroscience Studies, Queen's University, Kingston, Ontario K7L 3N6; and* [2]*Département de Physiologie, Université de Montréal, Montréal, Quebec H3C 3J7, Canada*

Submitted 29 August 2002; accepted in final form 22 January 2003

Graham, Kirsten M., Kimberly D. Moore, D. William Cabel, Paul L. Gribble, Paul Cisek, and Stephen H. Scott. Kinematics and kinetics of multijoint reaching in nonhuman primates. *J Neurophysiol* 89: 2667–2677, 2003. First published January 29, 2003; 10.1152/jn.00742.2002. The present study identifies the mechanics of planar reaching movements performed by monkeys (*Macaca mulatta*) wearing a robotic exoskeleton. This device maintained the limb in the horizontal plane such that hand motion was generated only by flexor and extensor motions at the shoulder and elbow. The study describes the kinematic and kinetic features of the shoulder, elbow, and hand during reaching movements from a central target to peripheral targets located on the circumference of a circle: the center-out task. While subjects made reaching movements with relatively straight smooth hand paths and little variation in peak hand velocity, there were large variations in joint motion, torque, and power for movements in different spatial directions. Unlike single-joint movements, joint kinematics and kinetics were not tightly coupled for these multijoint movements. For most movements, power generation was predominantly generated at only one of the two joints. The present analysis illustrates the complexities inherent in multijoint movements and forms the basis for understanding strategies used by the motor system to control reaching movements and for interpreting the response of neurons in different brain regions during this task.

INTRODUCTION

It has been more than 30 years since Ed Evarts (1967) initiated his pioneering studies on the activity of individual neurons in primary motor cortex (MI) of nonhuman primates performing behavioral tasks. The goal of these studies was to understand how MI controls movement by assessing the type of information represented in the discharge pattern of neurons. Sensibly, these initial studies examined movements with a single degree-of-freedom (dof): flexion/extension motions at the wrist. These and subsequent studies have shown how the discharge patterns of neurons in MI are related to muscle force, joint motion, and other features of the task such as impending movement direction (Evarts 1967; Fetz and Cheney 1980; Thach 1978; for review, see Porter and Lemon 1993).

While these single-joint tasks remain a popular and useful paradigm for addressing many issues in the neural basis of motor control, they cannot address several key control problems that arise when movements include a second joint. First, there is not a simple mapping between end-effector (i.e., the hand) and joint motions such that the magnitude of motion at each joint depends on hand movement direction and extent and initial limb geometry. Hand movement to a particular location in space can be attained using many different spatial trajectories by altering the timing of motion at the two joints. Second, there is not a simple mapping between motion and torque at each joint due to intersegmental dynamics (Hasan 1991; Hollerbach and Flash 1982; Zajac and Gordon 1989). Torque at one joint may lead to motion at other joints, and the magnitude of these interactions depends on limb geometry. In effect, the additional problem that arises when movements involve more than one joint is that the brain must carefully coordinate motor patterns at one joint with those at another to smoothly move the hand through space.

There have been many studies exploring the discharge of neurons in motor cortex of nonhuman primates during multijoint motor tasks, and yet these types of studies cannot easily address how this brain region is involved in coordinating motor patterns at different joints (for review, see Scott 2000). For technical reasons, most studies have only monitored hand motion or force applied at the hand so that neural responses can only be related to global features of the task (Georgopoulos et al. 1982; Kalaska et al. 1989; Scott and Kalaska 1997).

To address how neural activity in regions of the brain may be involved in coordinating movements at different joints, we developed a new experimental device called kinesiological instrument for normal and altered reaching movements (KINARM), which can both monitor and manipulate the physics of limb motion (Scott 1999). Movement with this device is limited to the horizontal plane involving flexion and extension motions at the shoulder and elbow, an arm orientation used extensively in human research (Buneo et al. 1995; Flanagan and Rao 1995; Gomi and Kawato 1996; Gribble and Ostry 1999; Karst and Hasan 1991; Sainburg et al. 1999; Shadmehr and Mussa-Ivaldi 1994; Theeuwen et al. 1994), making it easier to compare and contrast motor function between primate species. Preliminary reports of our work have illustrated a range of observations on how the mechanical properties of the limb and mechanical loads applied to the joints are represented in the activity patterns of neurons in MI (Cabel et al. 2001; Gribble and Scott 2002; Scott et al. 2001). The goal of the present study is to provide a more complete account of the kinesiology of reaching movements performed by nonhuman primates wearing the robotic device. The mechanics of limb

Address for reprint requests: S. H. Scott, Dept. of Anatomy and Cell Biology, Centre for Neuroscience Studies, Queen's University, Kingston, Ontario K7L 3N6, Canada (E-mail: steve@biomed.queensu.ca).

The costs of publication of this article were defrayed in part by the payment of page charges. The article must therefore be hereby marked "*advertisement*" in accordance with 18 U.S.C. Section 1734 solely to indicate this fact.

movements are described illustrating essential features of how coordinated movements of the shoulder and elbow move the hand to spatial targets. Patterns of motion and torque during multijoint movements have been described in a number of studies, although there has been no systematic descriptive on how these patterns vary with movement direction. The present study also presents several additional features on the mechanics of movement, including the influence of passive mechanical properties of the joints, and measures of joint power, a variable we have found to be informative for describing the mechanical properties of the limb (Scott et al. 2001). More importantly, this study provides a foundation for interpreting our studies on the response of neurons in MI during movement.

METHODS

Apparatus and behavioral task

Reaching movements were studied in three juvenile male rhesus monkeys (*Macaca mulatta*) with weights ranging from 5 to 7 kg. Monkeys were trained to sit in a primate chair and make reaching movements with their right arm while the left arm was unrestrained. All procedures were approved by the Queen's University Animal Care Committee based on the guiding principles of the Canadian Council on Animal Care.

Details of the experimental facility and robotic device (KINARM) used in the present study have been documented elsewhere (Scott 1999). In brief, custom-fitted troughs attached the upper arm and forearm of the monkey to the mechanical linkage. The hinge joints of the linkage were aligned to the centers of rotation of the shoulder and elbow and allowed for flexion and extension movements at each joint permitting movements of the whole limb in the horizontal plane. Monkeys were trained to maintain a pronated forearm position with the palm of their hand on the trough surface. Although not used in this experiment, torque motors attached to the linkage could apply loads to each joint independently. Encoders attached to the motors monitored motor position and, indirectly, shoulder and elbow position. Additional feedback of motor performance was provided by torque sensors attached to the motors and accelerometers positioned below the hand.

The basic behavioral task has been briefly described elsewhere (Scott et al. 2001). Each monkey performed reaching movements from a centrally located target to 1 of 16 peripheral targets equally spaced about the circumference of a circle with a 60-mm radius. Spatial targets were projected onto the horizontal plane at the level of the upper limb using a semitransparent mirror and a computer-controlled LCD projector. To initiate each trial, the monkey was required to maintain its hand within the central target area (8 mm radius) for 1.5–2.0 s. A peripheral target was then illuminated, and the monkey had to initiate a movement to the target within 500 ms. Once the movement was initiated, the monkey had to attain the target within 220–350 ms. Finally, the monkey was required to maintain its hand within the 12-mm-radius target area for another 1.5–2.0 s to receive a water reward. The targets were presented in a pseudorandom block design consisting of two separate sets, each containing eight of the 16 targets. One set included targets 3, 4, 5, 9, 12, 13, 15, and 16 (set 1), whereas the second set contained targets 1, 2, 6, 7, 8, 10, 11, and 14 (set 2; see Fig. 2*A*). Movements were divided in this manner so set 1 contained movements that spanned joint-torque space in an approximately uniform manner, useful for neural-based studies (Gribble and Scott 2002). Six repetitions of movements to each target were performed in each block, and in subsequent analyses, the first repetition of each block was excluded.

Experimental data were collected using custom-made data-acquisition software (LabView, National Instruments). Analog signals of electromyographic (EMG) activity and output from the torque sensors and accelerometers were sampled at 1,000 Hz for *monkey A* and at 4,000 Hz for *monkeys B* and *C*. Joint angles and velocities were sampled at approximately 200 Hz. All signals were subsequently aligned and resampled at 200 Hz. Analysis of the EMG activity will be described in a future report.

Data recording and signal processing

For the present study, we randomly selected movement data from 10 recording sessions (9 from neural recording sessions and 1 where only EMG was recorded) for each monkey from our database. Therefore the results are based on 50 movements to each respective target (10 recording sessions with 5 repeat trials each) for each monkey. Data analyses were all performed using MatLab software (MathWorks).

Shoulder angle was defined as the external angle between the upper arm and the frontal plane and elbow angle as the external angle between the upper arm and the forearm (see Scott 1999). Starting from the anatomical position, neutral joint position was defined with the arm abducted 90° where the arm fully extended to the side of the body. Positive angles and velocities were defined as forward rotation of the distal relative to the proximal segments (flexion). Positive torques were associated with the same direction (flexor torque). Position and acceleration signals were low-pass filtered at 10 Hz using a fourth-order zero phase lag Butterworth digital filter. Velocities and accelerations were computed by differentiating joint positions. All signals were time-aligned to movement onset, defined as 10% of peak tangential hand velocity or an acceleration threshold of 0.3 rad s^{-2}, whichever occurred first. Note that total movement time did not match the time constraints imposed for limb motion between central and peripheral targets that was used to reward the monkey. These latter times (220–350 ms) defined the time period when the monkey left the circular region defining start position and reached the circular region defining target location. Total movement time was longer because movement started before and ended after the hand passed through these target edges.

The passive joint torque-angle relationship was calculated for each monkey by applying constant-magnitude loads to each joint and monitoring limb movement while the monkey was anesthetized. While in the primate chair and with the arm in the device, the monkeys were sedated with valium (0.5 mg/kg im), ketamine (4 mg/kg im), or a combination of the two (*monkey A*: ketamine and valium; *monkey B*: ketamine only; *monkey C*: valium only) and then anesthetized with propofol (2.5 ml/kg iv). Loads were then applied by the torque motors to the shoulder or elbow joints for 4-s blocks. EMG activity was monitored from selective arm muscles to ensure no tonic muscle activity during this task. Joint position was defined from the last 2 s of each block. Cubic curves were fit to estimate the torque-angle relationship.

Time-varying active torques at the shoulder and elbow were computed based on the kinematics of the joints and the equations of motion governing the mechanical behavior of the limb and KINARM (see Scott 1999). These calculations considered the effects of the passive torque generated at the shoulder and elbow, described in the preceding text. Joint power was calculated by multiplying active torque with joint angular velocity (Winter 1990).

RESULTS

As observed in previous studies (Georgopoulos et al. 1981; Scott and Kalaska 1997; Turner et al. 1995), a characteristic of arm movements is that hand paths are relatively straight. Figure 1, *A–C* depicts mean hand trajectories for *monkeys A–C*, respectively, for reaching to each target. Peak hand velocities for each monkey are displayed as polar plots against movement direction in Fig. 1, *D–F*. The magnitude of peak hand velocity was also similar to all 16 targets and was comparable across

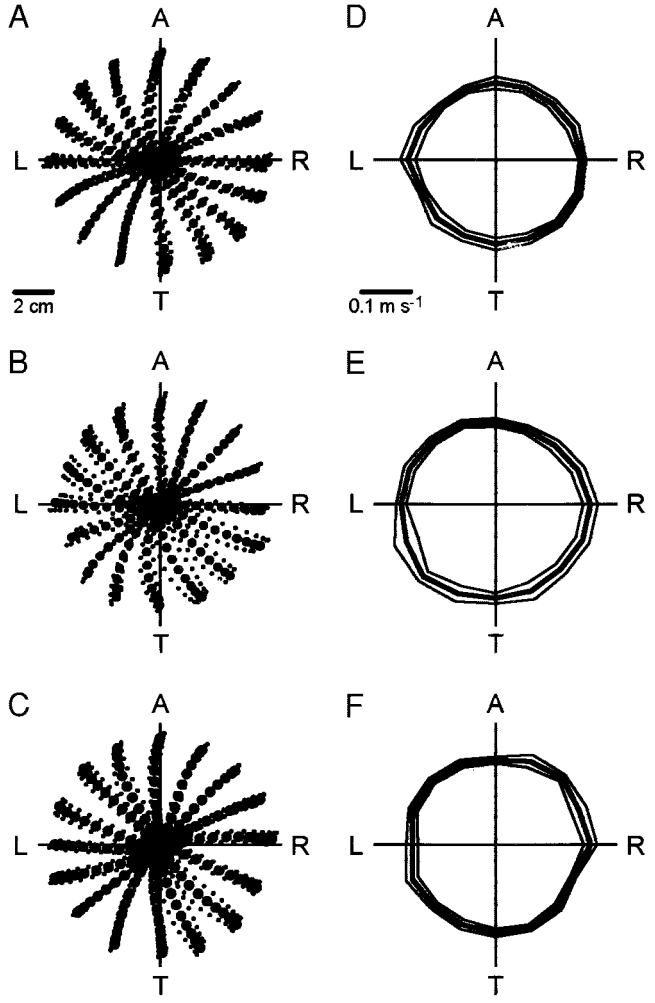

FIG. 1. Hand kinematics of movements in the workspace for all 3 monkeys. *A–C*: mean hand trajectories for *monkeys A–C*, respectively (means ± SD). ●, hand position at 40-ms increments. Movements were made in the horizontal plane away (A) and toward (T) the body, and to the left (L) and right (R) of a central target as well as intermediary directions. *D–F*: polar plots of peak hand velocity for *monkeys A–C*, respectively (means ± SD). Angle defines movement direction in Cartesian space and distance from origin defines the magnitude of peak hand velocity.

monkeys. Most of the following analyses focus on one representative subject (*monkey A*), but similar results were found in all monkeys.

Active torque and joint motion are tightly coupled for single-joint motor tasks. However, the coupling between torque and motion is more complex for multijoint movements due to intersegmental dynamics. Figure 2 depicts two examples to illustrate this point. Movements to target 2 (Fig. 2*C*) required motion at only the elbow but required similar active torque at the shoulder and elbow. In contrast, movements to target 15 (Fig. 2*D*) required similar motion at the two joints but only active torque at the shoulder. Although hand velocity was uniform for movements in different spatial directions (see Fig. 1, *D–F*), motion of the individual joints was highly anisotropic. Figure 3*A* illustrates peak shoulder and elbow velocity as polar plots, where direction defines target location and magnitude reflects absolute peak velocity. Figure 3, *C* and *D*, displays the temporal pattern of joint velocity at the shoulder and elbow, respectively, for movements in different spatial directions. The diagrams are spatial maps displaying the instantaneous velocity of the joint at each location in hand space from the start position (the center of the diagram) to each peripheral target location (the perimeter of the circle). Movements toward and away from the body required the largest angular velocities at the elbow, whereas movements to the left or right required far less angular motion. The greatest angular velocities at the shoulder occurred for movements at approximately 110 and 290° (targets 6 and 14) and at approximately 90 and 270° (targets 5 and 13) for the elbow. When total motion at the two joints was considered, there was more than a fourfold variation in the combined rotation at the shoulder and elbow joints when reaching across all spatial directions. This large variation in joint velocities for movements in different spatial directions simply reflects the geometric relationship between joint and hand motion, as shown in Fig. 3*B*. This diagram illustrates the instantaneous velocity of the hand for movements along the principal axes. It also displays the associated contribution of shoulder and elbow motion to hand velocity at the mid-point of the movement. Motion at either joint tends to move the hand to the left or right (see DISCUSSION).

Although Fig. 3, *A* through *D* plot joint velocities relative to the spatial direction of hand motion, it is also useful to plot joint motion in joint-based coordinate frames. Figure 3*E* illustrates changes in joint angle for each movement. While the diagram reiterates the previous point that total angular motion varied across movement directions, it is important to note that all but 2 of the 16 movement directions were located in two of the four quadrants of joint-angle space. All movements toward the body required combined elbow flexion and shoulder extension, whereas all movements away from the body required combined elbow extension and shoulder flexion. Movements principally to the right or left (targets 2 and 9) were the only directions that required combined extension or combined flexion, respectively, at both joints. Another point illustrated in this figure is that changes in joint motion remained relatively constant throughout movement. This can be best seen in Fig. 3*F* where changes in shoulder velocity tended to parallel changes in elbow velocity, illustrating the consistency with which movements at the two joints were coordinated together.

Each monkey's arm was manipulated passively by the robotic device to determine the passive mechanical properties of the joints (Fig. 4, *A* and *B*). These position-dependent passive properties of the shoulder and elbow were fit with a cubic function for each monkey (Table 1). The black arrows denote arm geometry at the central target where there was minimal passive force at either joint (shoulder angle = 0.57 rad; elbow angle = 1.47 rad). From this position, passive torques grew exponentially when the joint was either flexed or extended. Predictions of the passive torque at the shoulder and elbow at each hand location within the workspace are plotted in Fig. 4, *C* and *D*, respectively. The center of the diagram reflects the central start position and the solid circles represent the peripheral targets. Maximal passive torque generated at the joints during the reaching task was around 0.1 N m and not surprisingly occurred for movements away and toward the body. The magnitude of these passive forces varied somewhat between monkeys.

As observed with joint motion (see Fig. 3*A*), peak active torque at the shoulder and elbow varied strongly with movement direction (Fig. 5*A*), although there were some important

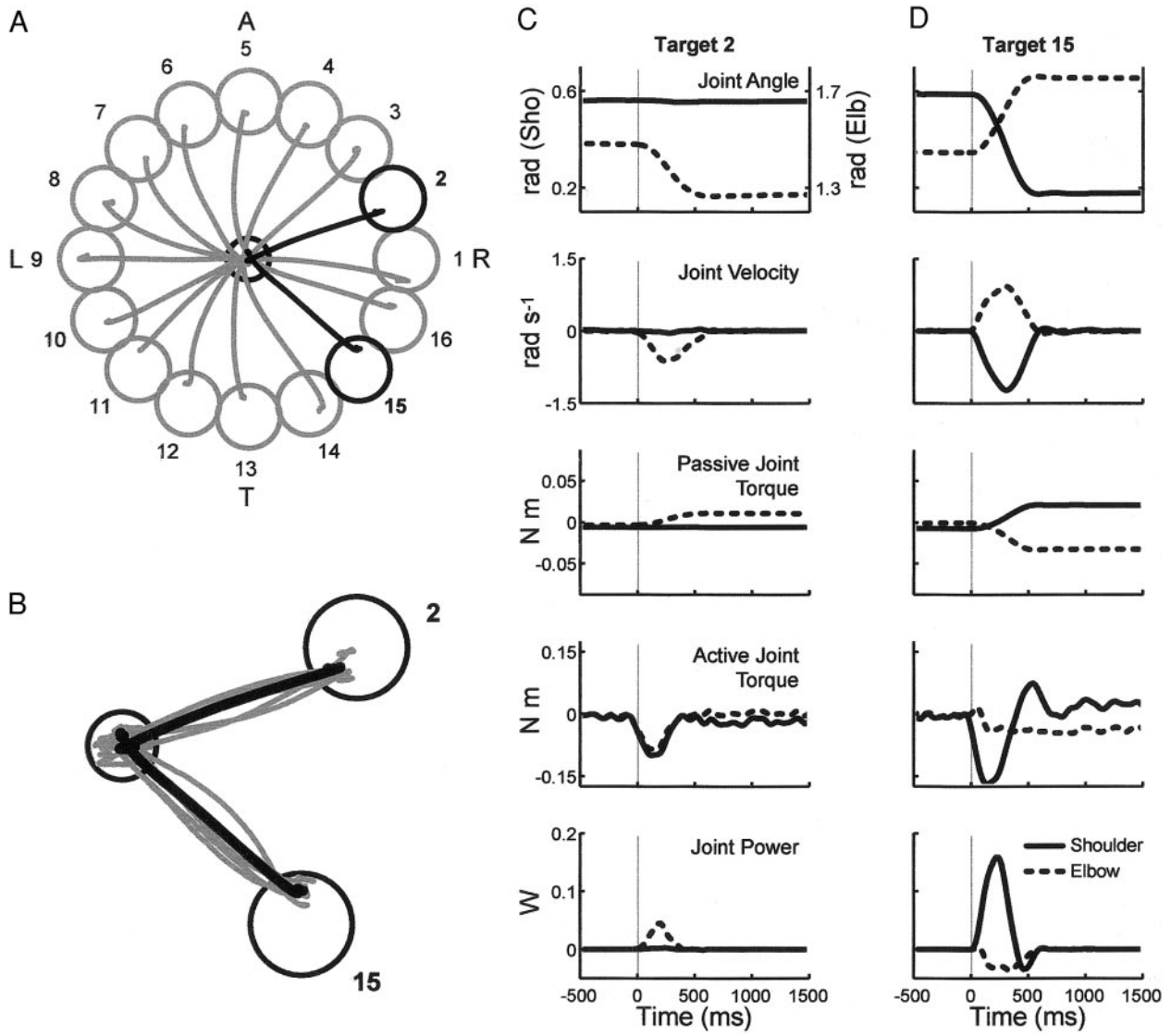

FIG. 2. Kinematic and kinetic features of 2 of the 16 reaching movements for *monkey A. A*: average hand trajectories for 5 movements from the central start position to each of the 16 peripheral targets. Targets 2 and 15 (black lines) are used as examples in the following panels to illustrate some biomechanical features of reaching. *B*: hand trajectories from 5 repeat reaching trials to targets 2 and 15 (gray lines). Average hand trajectories are superimposed (black lines). *C* and *D*: changes in joint angle, velocity, passive and active torque, and power at the shoulder (solid lines) and elbow (dashed lines) when moving to targets 2 (*C*) and 15 (*D*). Vertical gray lines depict movement onset.

differences. First, peak torque was not aligned with movement directions associated with the largest angular velocities. Shoulder and elbow torque were maximal in the opposite quadrants, such that movement directions associated with the greatest shoulder torque, 158 and 315° (targets 8 and 15), were orthogonal to the directions requiring the greatest elbow torque: 45 and 225° (targets 2 and 11). Second, the magnitude of torque at the elbow was generally smaller than that at the shoulder even though peak angular velocities were similar for the two joints.

Spatial maps of the instantaneous active torque for the shoulder and elbow at each hand location are displayed in Fig. 5, *B* and *C*, respectively. These diagrams illustrate that breaking torques to stop hand motion were smaller than the initial torques to start movement, particularly at the elbow. Initial torque at the elbow did not have a discernable burst due to the gradual increase in passive joint forces throughout movement. As a result, elbow torque looked more like a ramp-and-hold motor response rather than the phasic pattern observed at the shoulder. These temporal responses reflect the modest movement speed in our task, the influence of passive torque generated at each joint (particularly at the elbow), and the viscous properties of the robotic linkage.

Figure 5*D* depicts joint torque for each of the 16 targets plotted in joint-torque space. Whereas velocity tended to be distributed in the elbow flexion-shoulder extension and elbow extension-shoulder flexion quadrants (see Fig. 3*E*), torque showed the opposite pattern although it was less distinct. Many movement directions initially required either combined flexor torques or combined extensor torques. As well, joint torque in

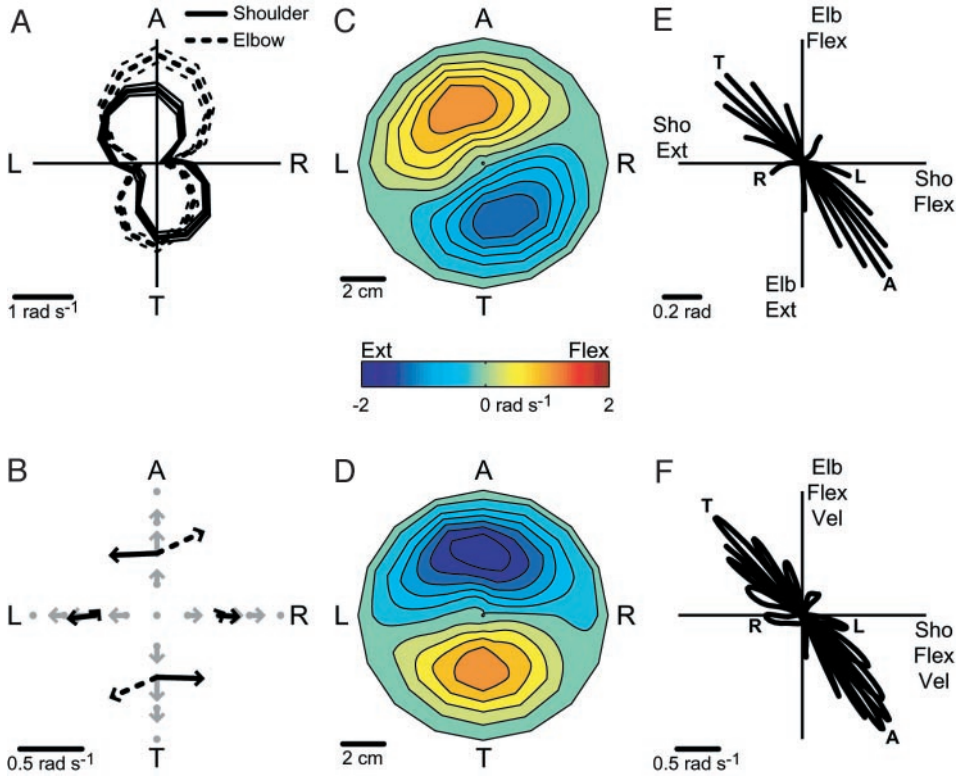

FIG. 3. Joint kinematics of reaching for *monkey A. A*: polar plot of peak shoulder (solid lines) and elbow (dashed lines) velocity where angle defines movement direction in Cartesian space and length defines magnitude of peak joint velocity (means ± SD). *B*: hand-velocity vectors (gray arrows), along with shoulder (solid black arrows) and elbow vectors (dashed black arrows) reflecting their contribution to hand velocity during reaching in 4 directions. *C* and *D*: spatial maps reflecting the instantaneous velocity of the shoulder (*C*) and elbow (*D*) at each location in space during the task. The center of the diagram is start position and the perimeter is the peripheral target locations. *E*: changes in joint angle plotted in joint-angle coordinates for each movement direction. *F*: joint velocity for movement to each target of the reaching paradigm plotted in joint-velocity space.

these quadrants tended to be scaled, that is, the temporal patterns of active torque at the two joints were similar. In contrast, shoulder and elbow torque for movement directions falling in the other two quadrants were much less coupled, illustrated by large loops in these quadrants.

Single-joint movements possess a simple one-to-one mapping between motion and torque at a joint. Multijoint movements distort this mapping as illustrated in Fig. 6 where peak active torque is plotted against peak joint acceleration for all movements examined in this study. While there was a reasonably strong correlation between acceleration and torque at the shoulder ($r^2 = 0.75$), it was by no means a perfect mapping. The correlation between elbow acceleration and torque was much weaker ($r^2 = 0.38$), and, in many cases, the sign of elbow torque was opposite to that of elbow acceleration (top left and bottom right quadrants). In other words, the observed motion of the joint did not necessarily match the underlying active torque being generated at that joint and, in some cases, the torque was even the opposite sign (i.e., flexor motion occurred with an extensor torque).

Power is a more complex variable than either velocity or torque because one can have positive or negative power being generated or absorbed at a joint and by either the flexors or extensors (Winter 1990). Figure 7 plots the magnitude of power at the two joints for each movement. Positive power reflects generation of energy that is transmitted to the limb by the shoulder (*x* axis) or elbow (*y* axis), whereas negative power reflects energy dissipation or removal at a given joint. Perhaps the most striking feature is that power generation tended to occur at only one of the two joints with rather abrupt shifts in power production between adjacent target directions. For example, the shoulder provided all the power for movements to target 1, whereas the elbow provided all the power for movements to target 2. In only a few directions is substantial power generated at both joints (targets 5, 6, 7, 13 and 14). Interestingly, when both joints contributed to power generation their temporal patterns were shifted. For targets 5–7, the shoulder generated power initially, followed by the elbow's contribution. The reverse pattern was observed for targets 13 and 14.

Joint power was highly anisotropic where peak values occurred for movements away and to the left, and toward and to the right (Fig. 8*A*). Not surprisingly, directions requiring the greatest power tended to fall between directions requiring maximal velocity and torque at each joint. Maximum shoulder power occurred at 135 and 293° (targets 7 and 14), whereas elbow power reached its maximum at 90 and 248° (targets 5 and 12). Figure 8, *B* and *C*, displays the instantaneous power at the shoulder and elbow, respectively, at each hand location from the central target (center) to the peripheral targets (perimeter of diagram). Due to passive joint properties and the dissipative properties of the robot, joint power was largely positive throughout movement.

DISCUSSION

Single-joint, single DOF movements maintain a simple mapping between joint and endpoint motion and between joint kinematics and kinetics. By adding one additional joint to the system, there is an abrupt shift in mechanical complexity such that these simple mappings no longer exist. Consequently, it is substantially more challenging to intuitively predict and understand the physics of limb motion. The purpose of the present study is to provide a description of limb mechanics for a commonly studied arm movement paradigm, the center-out task.

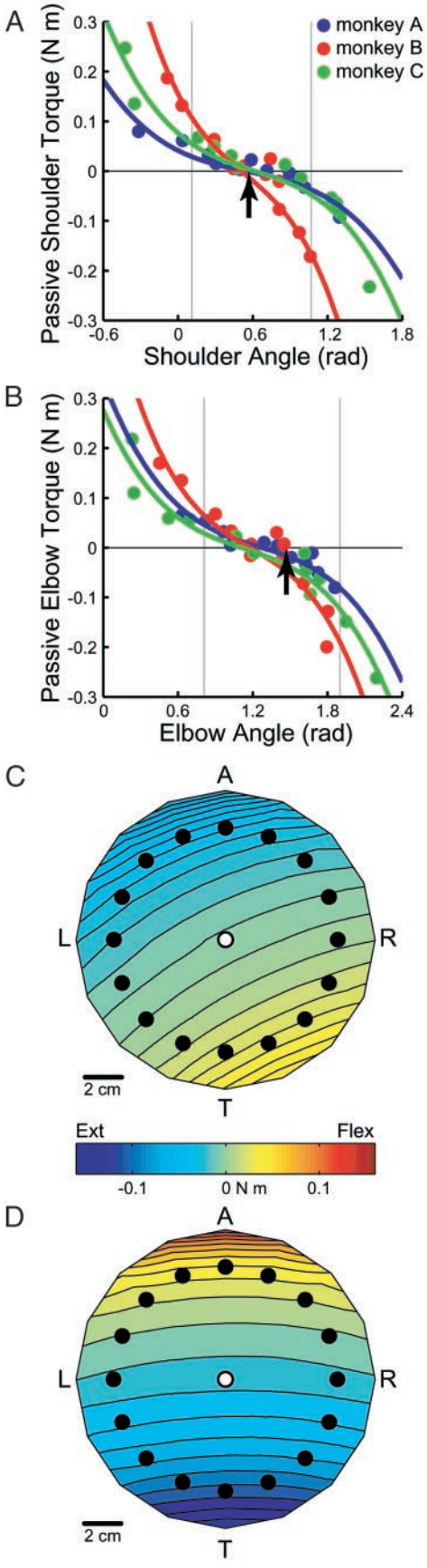

FIG. 4. Passive joint properties for the 3 monkeys. *A* and *B*: joint angle for *monkeys A* (blue), *B* (red), and *C* (green) when various magnitudes of torque are applied to the shoulder (*A*) and elbow (*B*) along with fitted cubic polynomial (for coefficients, see Table 1). The joint-angle range when reaching in the present task is represented by vertical gray lines. Black arrows indicate joint position at the central target. *C* and *D*: loads experienced by the shoulder (*C*) and elbow (*D*) by *monkey A* when moving throughout the workspace. The open circle denotes the central start position and solid circles represent the location of the 16 targets in the reaching paradigm.

TABLE 1. *Polynomial* coefficients for passive mechanical joint properties*

Monkey	*a*	*b*	*c*	*d*
		A. Shoulder		
A	−0.08	0.13	−0.13	0.04
B	−0.33	0.52	−0.49	0.16
C	−0.13	0.23	−0.22	0.08
		B. Elbow		
A	−0.12	0.46	−0.65	0.34
B	−0.23	0.82	−1.11	0.55
C	−0.13	0.44	−0.58	0.28

* $y = ax^3 + bx^2 + cx + d$.

Limb mechanics during reaching

It is easy to move one's own limb to qualitatively identify that hand movements starting in the middle of the workspace and in the sagittal plane require motion at both the shoulder and elbow, movements at the shoulder alone generate hand motion to the left or right, and movements at the elbow generate hand motion to the right and up, and to the left and down. What is somewhat surprising, however, is that sagittal plane movements require four times as much total motion at the two joints as compared with frontal plane movements even when hand movement distance is identical (Fig. 3*E*).

This apparent "inefficiency" for sagittal-plane movements can be best explained by examining how motion at each joint contributes to endpoint (hand) movement. Figure 3*B* displays the instantaneous velocity of the hand for movements along the principal axes. The diagram also illustrates how shoulder and elbow motion contributes to hand velocity at the mid-point of the movement. Movements to the left and right were created almost exclusively by motion at the shoulder because its contribution to endpoint movement is oriented largely in this plane. In contrast for movements in the sagittal plane, a substantial amount of angular motion is required to counteract out-of-plane movement. For movements away from the body, elbow extension contributes to hand motion both away and substantially to the right. This rightward motion is compensated for by shoulder motion which tends to move the hand to the left. Therefore joint motion tends to contribute largely to movement in the frontal plane providing only a small contribution to hand motion along the intended sagittal direction. This inefficiency becomes even more extreme as the limb becomes more fully extended.

Another important characteristic of the mapping between hand and joint motion is that while hand motion was uniformly distributed in Cartesian space in our task, motion at the joints almost always required flexion at one joint combined with extension at the other (Fig. 3*E*). Only 2 of the 16 directions

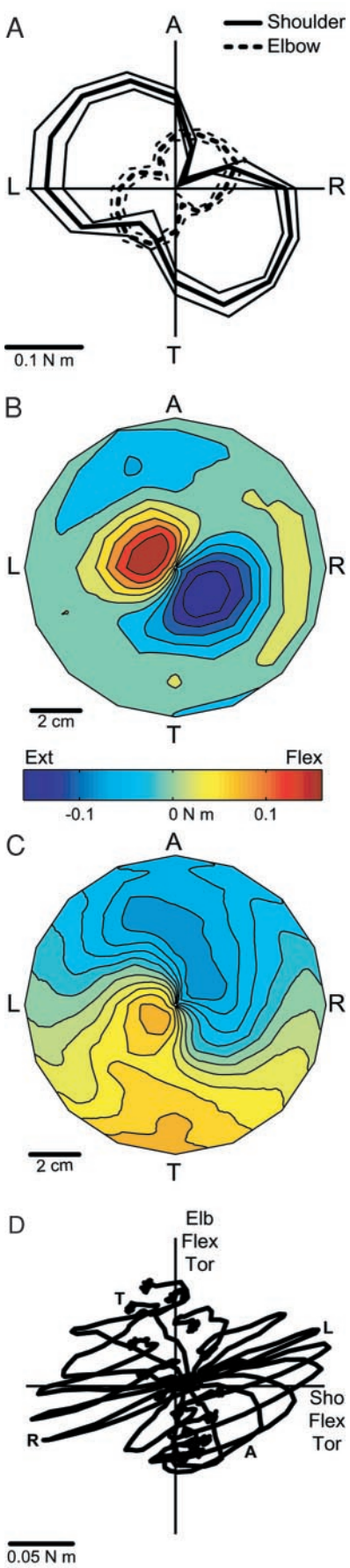

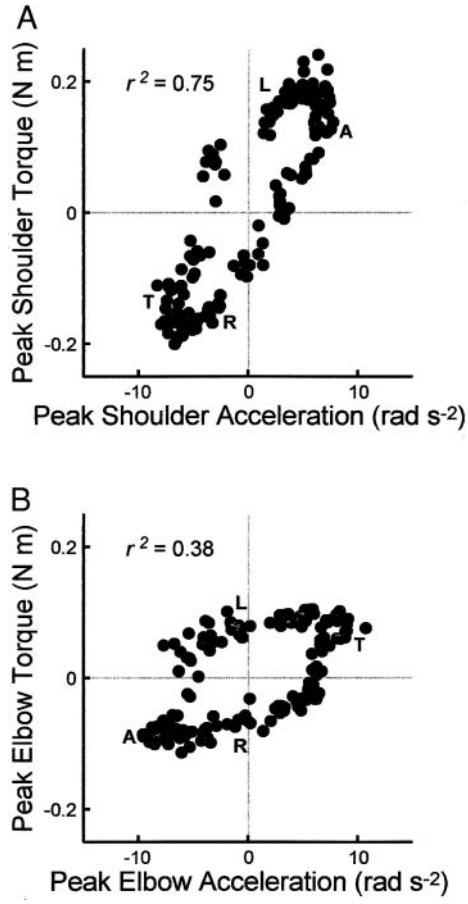

FIG. 6. Distortion in the mapping between motion and torque at each joint due to intersegmental forces. Correlation between peak joint acceleration and peak joint torque for shoulder (*A*) and elbow (*B*) during 10 recording sessions for *monkey A.*

involved motion of similar sign at the two joints, termed whipping movements by Hollerbach and Flash (1982). These anisotropies in joint motion have a number of important implications regarding motor performance, particularly how temporal or spatial deviations in angular motion translate into endpoint errors. In general, small deviations in joint motion for sagittal plane hand movements lead to larger endpoint errors than similar sized deviations for movements in the frontal plane. These anisotropies between hand and joint motion also influence proprioceptive estimates of hand position from muscles spindles (Scott and Loeb 1994).

As illustrated in the results, the underlying mechanics of movement are quite different from the overlying joint motions. First, there are substantial differences in how motion and torque vary with movement direction (Figs. 3*A* and 5*A*). Anisotropies of angular motion at the shoulder and elbow are similar in direction and in magnitude. In contrast, anisotropies of active torque at the shoulder and elbow are perpendicular to

FIG. 5. Joint torque during reaching movements of *monkey A. A*: polar plots of maximum shoulder (—) and elbow (- - -) torque, where angle defines movement direction in Cartesian space and length defines magnitude of peak joint torque (means ± SD). *B* and *C*: spatial maps reflecting the instantaneous active torque at the shoulder (*B*) and elbow (*C*) at each location in space during the task. The center of the diagram is start position and the perimeter is the peripheral target locations. *D*: active joint torque profiles for each movement direction plotted in joint-torque space.

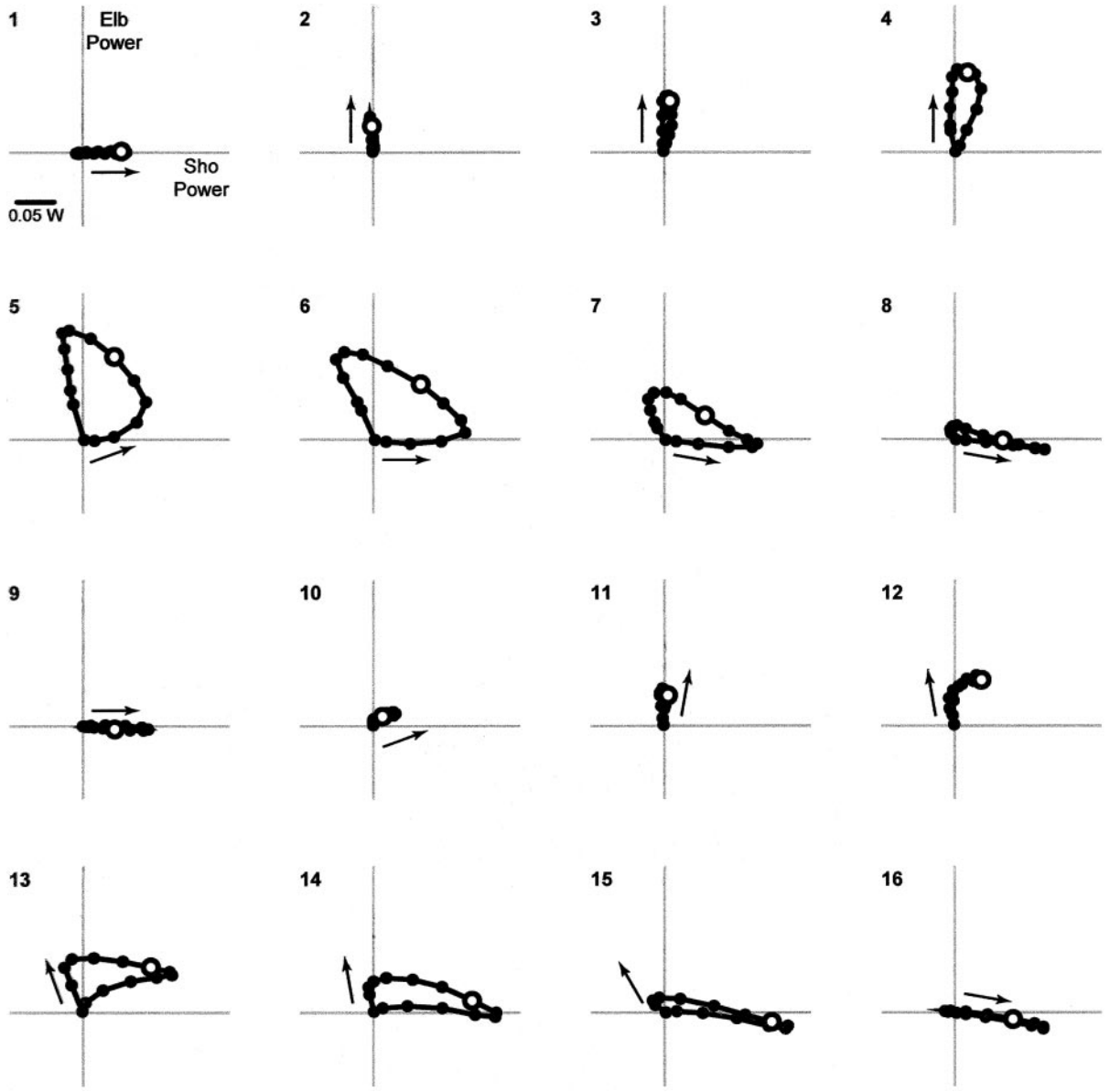

FIG. 7. Joint power for individual target locations plotted in joint-power space for *monkey A*. ●, 40-ms time intervals; ○, time at which peak tangential hand velocity is attained. ↑, the direction of initial power generation. Positive and negative power reflects energy generation or dissipation, respectively, at the shoulder (*x* axis) and/or elbow (*y* axis).

each other and the shoulder torques tend to be larger in magnitude. These patterns of active torque are smaller in magnitude but qualitatively similar to humans (Buneo et al. 1995). Second, most movements initially require combined flexor torques or combined extensor torques (Fig. 5*D*) in spite of the fact that the overlying motion at the joints was often opposite in sign. That is, it was relatively common to have flexor motion and extensor torque, or vice versa, at one of the two joints. These apparent inconsistencies between motion and torque at a given joint simply reflects limb mechanics and illustrate why it is difficult to intuitively predict underlying torques from the observed motion of the limb.

The large difference between motion and torque at each joint is one reason why joint power provides a valuable description of motor performance. Joint power has been used extensively in the locomotion field to describe the action of joints in the lower limb (Eng et al. 1997; Johnson and Buckley 2001; Robertson and Winter 1980; Winter 1983) but has been less commonly used for upper limb research (Hatzitaki and Hoshizaki 1998; Scott et al. 2001). Joint power describes the transfer of energy into and out of the limb generated by muscles spanning each joint. A particularly surprising observation is that for most movements, power is almost exclusively generated at only one of the two joints (Fig. 7). This pattern occurs because either active torque or joint velocity often approaches zero at one of the two joints resulting in the other joint providing the bulk of power to initiate movement. In situations where both joints contributed substantially to joint power, their temporal patterns tended to be different resulting in power generation at one joint followed by generation at the other. This contrasts with joint motion where temporal patterns were often similar at both joints (Figs. 3*F*).

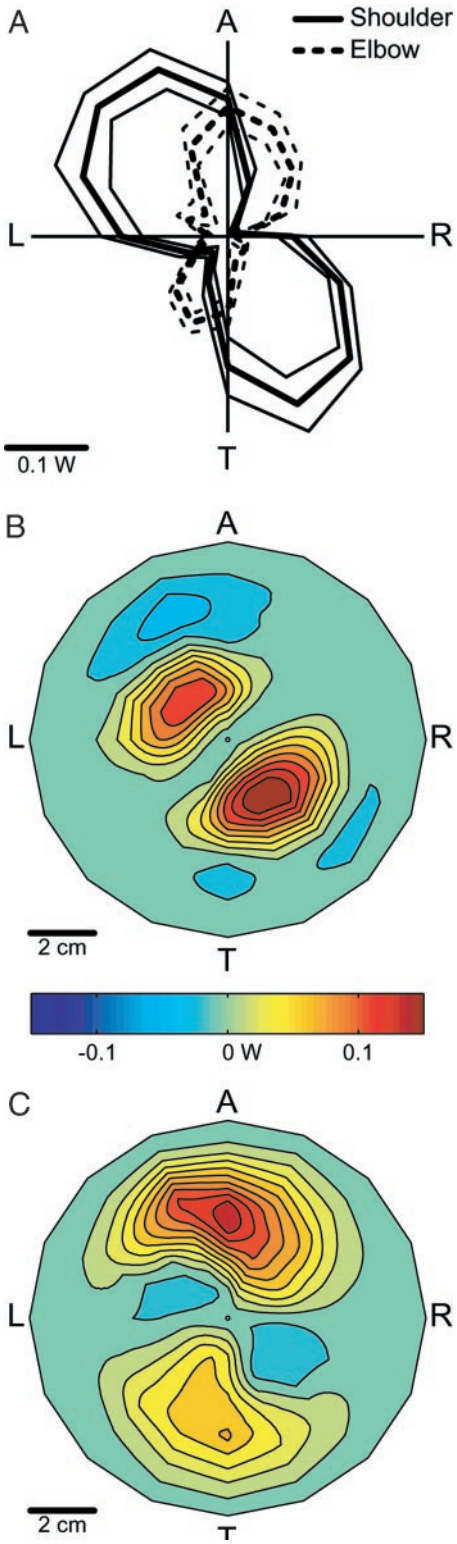

FIG. 8. Joint power during reaching for *monkey A. A*: peak shoulder (—) and elbow (- - -) power, where angle defines movement direction in Cartesian space and length defines magnitude of peak joint power (means ± SD). *B* and *C*: spatial maps reflecting the instantaneous power at the shoulder (*B*) and elbow (*C*) at each location in space during the task. The center of the diagram is start position and the perimeter is the peripheral target locations.

In addition to providing a measure of energy flow into and out of the limb, joint power provides at least a first approximation of muscle activity during movement. A major factor that influences muscle force production is muscle velocity as defined by the classic force-velocity relationship of muscle (Hill 1938; Scott et al. 1996). If a muscle shortens, it generates less force than under isometric conditions, whereas if it lengthens, it can generate more force. Power reflects change in muscle activity from isometric levels because it increases with velocity if torque is the same sign and decreases if they are opposite in sign. This ability to approximate muscle activation is likely why we found a correlation between joint power and the distribution of preferred directions of neurons in MI (Scott et al. 2001). However, joint power does not reflect muscle activity well for isometric or slow movements where velocity approaches zero and active torque would probably better reflect muscle activation in this case, assuming no significant co-contraction of antagonist muscles. A blend between torque and power could be a beneficial variable to reflect the effective activity of a muscle group although some scaling between these variables would be necessary. Our future work will examine more fully the relationship between muscle activity, and joint motion, torque and power during movement.

Implications for neural control

There are two different hypotheses on how motor patterns at the shoulder and elbow are coordinated together to generate reaching movements. It has been proposed that subjects use a simple scaling strategy such that torque (and EMG) at the two joints are synchronized with similar patterns of torque (Gottlieb et al. 1996). Alternatively, others suggest that movements in different spatial directions result in systematic shifts in onset time creating temporal shifts in the pattern of torques (and EMG) at the two joints (Karst and Hasan 1992; Wadman 1980) and even among muscles at a given joint (Flanders et al. 1994; Hoffman and Strick 1999). Our data on nonhuman primates during multijoint movements support both strategies depending on movement direction. We found clear temporal shifts in torque (Fig. 5*D*) and power (Fig. 7, movements 5, 6, 7, 13, and 14) for movements toward and away from the monkey. In contrast, movements to the right and left showed fairly simple scaling patterns of active torque at the two joints (Fig. 5*D*). These latter movements roughly match the directions of sagittal-plane movement examined by Gottlieb et al. (1996) where scaling of torque patterns was observed in humans. This suggests that the CNS may use both strategies depending on task conditions, such as movement direction.

As well, we found evidence that while torque patterns may be scaled for movements predominantly to the left or right, the associated power generated at each joint did not scale. In general, only one of the two joints provided substantial power to the limb during these multi-joint movements (Fig. 7), suggesting more of a single-joint strategy for controlling multi-joint movement. Our recent human-based study also show power generation at only one joint to initiate multi-joint planar movements in naïve subjects (Rombough et al. 2002).

Variations in movement speed were not observed in this study, although a previous study on nonhuman primates have found variations in hand velocity with movement direction

(Turner et al. 1995), and human studies have also documented consistent variations in velocity (Gordon et al. 1994; Rombough et al. 2002). A key difference in our study is that movements between the central and peripheral targets were required to be no faster than 220 ms and no slower than 350 ms (note that total movement time is actually longer; see METHODS) and the monkeys learned to perform these movements with a high success rate (approximately 95%). While variations in movement speed with movement direction could still have occurred within this limited time period, there was no evident variation. This suggested that these animals had more fully compensated for the mechanical properties of the limb (and KINARM) when moving to different spatial targets due to the experimental design as compared with naive human subjects performing similar tasks.

An important question is how much of the present observations could be predicted from a simple mechanical model of the arm and assumptions about straight hand paths and bell-shaped hand-velocity profiles. Although not the focus of this article, hand trajectories were not perfectly straight and showed small variations dependent on movement direction (Fig. 1). Such variations from straight hand trajectories will not substantially influence patterns of joint velocity. However, we expect that these small variations will influence the estimated joint torques and powers and thus reflect to some degree the underlying motor strategies for reaching, as described in the preceding text. In particular, the observation that joint power tends to occur at only one of the two joints is unlikely to simply reflect straight hand paths and bell-shaped velocity profiles. Our future work using mathematical models to simulate limb movements will assess this issue more fully.

Neural computations associated with converting spatial information of target location into muscle activity can be viewed as an internal model of the limb, a neural process that mimics its physical properties (Kalaska et al. 1997; Kawato et al. 1987). This notion of internal models for motor control was instrumental in guiding our recent neural studies illustrating how neural activity in primary motor cortex of nonhuman primates is influenced by limb mechanics (Scott et al. 2001) as well as joint-based loads during posture and movement (Cabel et al. 2001; Gribble and Scott 2002). Therefore while the present data are descriptive in nature, their presentation highlights important principles on Newtonian mechanics as well as motor strategies that primates use to perform reaching movements. We believe such information on the motor periphery is essential for understanding central processing to coordinate movement.

The authors thank M.-J. Bourque at Université de Montréal for expert technical assistance. S. Chan assisted in the training of one monkey.

This research was supported by Canadian Institutes of Health Research (CIHR) Grant MT-13462 and a Medical Research Council scholarship to S. H. Scott. P. L. Gribble was supported by a CIHR Postdoctoral Fellowship and P. Cisek was supported by a scholarship from the National Institutes of Health.

Present address of P. L. Gribble: Dept. of Psychology, The University of Western Ontario, London, Ontario N6A 5C2, Canada.

REFERENCES

Buneo CA, Boline J, Soechting JF, and Poppele RE. On the form of the internal model for reaching. *Exp Brain Res* 104: 467–479, 1995.

Cabel DW, Cisek P, and Scott SH. Neural activity in primary motor cortex related to mechanical loads applied to the shoulder and elbow during a postural task. *J Neurophysiol* 86: 2102–2108, 2001.

Eng JJ, Winter DA, and Patla AE. Intralimb dynamics simplify reactive control strategies during locomotion. *J Biomech* 30: 581–588, 1997.

Evarts EV. Representation of movements and muscles by pyramidal tract neurons of the precentral motor cortex. In: *Neurophysiological Basis of Normal and Abnormal Motor Activities*, edited by Yahr MD and Purpura DP. New York: Raven, 1967, p. 215–253.

Fetz EE and Cheney PD. Postspike facilitation of forelimb muscle activity by primate corticomotoneuronal cells. *J Neurophysiol* 44: 751–772, 1980.

Flanagan JR and Lolley S. The inertial anisotropy of the arm is accurately predicted during movement planning. *J Neurosci* 21: 1361–1369, 2001.

Flanagan JR and Rao AK. Trajectory adaptation to a nonlinear visuomotor transformation: evidence of motion planning in visually perceived space. *J Neurophysiol* 74: 2174–2178, 1995.

Flanders M, Pellegrini JJ, and Soechting JF. Spatial/temporal characteristics of a motor pattern for reaching. *J Neurophysiol* 71: 811–813, 1994.

Georgopoulos AP, Kalaska JF, Caminiti R, and Massey JT. On the relations between the direction of two-dimensional arm movements and cell discharge in primate motor cortex. *J Neurosci* 2: 1527–1537, 1982.

Georgopoulos AP, Kalaska JF, and Massey JT. Spatial trajectories and reaction times of aimed movements: effects of practice, uncertainty, and change in target location. *J Neurophysiol* 46: 725–743, 1981.

Gomi H and Kawato M. Equilibrium-point control hypothesis examined by measured arm stiffness during multijoint movement. *Science* 272: 117–120, 1996.

Gordon J, Ghilardi MF, Cooper SE, and Ghez C. Accuracy of planar reaching movements. II. Systematic extent errors resulting from inertial anisotropy. *Exp Brain Res* 99: 112–130, 1994.

Gottlieb GL, Song Q, Hong DA, and Corcos DM. Coordinating two degrees of freedom during human arm movement: load and speed invariance of relative joints torques. *J Neurophysiol* 76: 1–11, 1996.

Gribble PL and Ostry DJ. Compensation for interaction torques during single- and multijoint limb movement. *J Neurophysiol* 82: 2310–2326, 1999.

Gribble PL and Scott SH. Overlap of internal models in motor cortex for mechanical loads during reaching. *Nature* 417: 938–941, 2002.

Hasan Z. Biomechanics and the study of multijoint movements. In: *Motor Control: Concepts and Issues*, edited by Humphrey DR and Freund H.-J. New York: Wiley, 1991, p. 75–84.

Hatzitaki V and Hoshizaki TB. Dynamic joint analysis as a method to document coordination disabilities associated with Parkinson's disease. *Clin Biomech* 13: 182–189, 1998.

Hill AV. The heat of shortening and the dynamic constants of muscle. *Proc R Soc Lond B Biol Sci* 126: 136–195, 1938.

Hoffman DS and Strick PL. Step-tracking movements of the wrist. IV. Muscle activity associated with movements in different directions. *J Neurophysiol* 81: 319–333, 1999.

Hollerbach MJ and Flash T. Dynamic interactions between limb segments during planar arm movement. *Biol Cybern* 44: 67–77, 1982.

Johnson MD and Buckley JG. Muscle power patterns in the mid-acceleration phase of sprinting. *J Sports Sci* 19: 263–272, 2001.

Kalaska JF, Cohen DA, Hyde ML, and Prud'homme M. A comparison of movement direction-related versus load direction-related activity in primate motor cortex, using a two-dimensional reaching task. *J Neurosci* 9: 2080–2102, 1989.

Kalaska JF, Scott SH, Cisek P, and Sergio LE. Cortical control of reaching movements. *Curr Opin Neurobiol* 7: 849–859, 1997.

Karst GM and Hasan Z. Initiation rules for planar, two-joint arm movements: agonist selection for movements through the workspace. *J Neurophysiol* 66: 1579–1593, 1991.

Kawato M, Furukawa K, and Suzuki R. A hierarchical neural-network model for control and learning of voluntary movement. *Biol Cybern* 57: 169–185, 1987.

Mussa-Ivaldi FA, Hogan N, and Bizzi E. Neural, mechanical, and geometric factors subserving arm posture in humans. *J Neurosci* 5: 2732–2743, 1985.

Porter R and Lemon RN. *Cortical Function and Voluntary Movement.* Oxford: Clarendon, 1993.

Robertson DG and Winter DA. Mechanical energy generation, absorption and transfer amongst segments during walking. *J Biomech* 13: 845–854, 1980.

Rombough SR, Flanagan JR, and Scott SH. Trajectory constraints in multidirectional whole-arm movements. *Soc Neurosci Abstr* 28: 767.3, 2002.

Sainburg RL, Ghez C, and Kalakanis D. Intersegmental dynamics are controlled by sequential anticipatory, error corrections, and postural mechanisms. *J Neurophysiol* 81: 1045–1056, 1999.

Scott SH. Apparatus for measuring and perturbing shoulder and elbow joint positions and torques during reaching. *J Neurosci Methods* 89: 119–127, 1999.

Scott SH. Role of motor cortex in coordinating multi-joint movements: is it time for a new paradigm? *Can J Physiol Pharmacol* 78: 923–933, 2000.

Scott SH, Brown IE, and Loeb GE. Mechanics of feline soleus: I. effect of fascicle length and velocity on force output. *J Muscle Res Cell Motil* 17: 207–219, 1996.

Scott SH, Gribble PL, Graham KM, and Cabel DW. Dissociation between hand motion and population vectors from neural activity in motor cortex. *Nature* 413: 161–165, 2001.

Scott SH and Kalaska JF. Reaching movements with similar hand paths but different arm orientations. I. Activity of individual cells in motor cortex. *J Neurophysiol* 77: 826–852, 1997.

Scott SH and Loeb GE. The computation of position sense from spindles in mono- and multiarticular muscles. *J Neurosci* 14: 7529–7540, 1994.

Shadmehr R and Mussa-Ivaldi FA. Rapid adaptation to coriolis force perturbations of arm trajectory. *J Neurosci* 14: 3208–3224, 1994.

Thach WT. Correlation of neural discharge with pattern and force of muscular activity, joint position, and direction of intended next movement in motor cortex and cerebellum. *J Neurophysiol* 41: 654–676, 1978.

Theeuwen M, Gielen CCAM, Miller LE, and Doorenbosch C. The relation between the direction dependence of electromyographic amplitude and motor unit recruitment thresholds during isometric contractions. *Exp Brain Res* 98: 488–500, 1994.

Turner RS, Owens JW, Jr., and Anderson ME. Directional variation of spatial and temporal characteristics of limb movements made by monkeys in a two-dimensional work space. *J Neurophysiol* 74: 684–697, 1995.

Wadman WJ, Denier van der Gon JJ, and Derksen RJA. Muscle activation patterns for fast goal-directed arm movements. *J Human Movement Studies* 6: 19–37, 1980.

Winter DA. Moments of force and mechanical power in jogging. *J Biomech* 16: 91–97, 1983.

Winter DA. *Biomechanics and Motor Control of Human Movement.* New York: Wiley, 1990.

Zajac FE and Gordon ME. Determining muscle's force and action in multi-articular movement. *Exer Sport Sci Rev* 17: 187–230, 1989.